ACS Medicinal Chemistry Letters

pubs.acs.org/acsmedchemlett Letter

Steroid–Quinoline Hybrids for Disruption and Reversion of Protein Aggregation Processes

Published as part of the ACS Medicinal Chemistry Letters virtual special issue "Medicinal Chemistry in Portugal and Spain: A Strong Iberian Alliance".

Hélio M. T. Albuquerque,[#] Raquel Nunes da Silva,[#] Marisa Pereira, André Maia, Samuel Guieu, Ana Raquel Soares, Clementina M. M. Santos, Sandra I. Vieira, and Artur M. S. Silva*

Cite This: *ACS Med. Chem. Lett.* 2022, 13, 443–448 Read Online

ACCESS | Metrics & More | Article Recommendations | Supporting Information

ABSTRACT: Reversing protein aggregation within cells may be an important tool to fight protein-misfolding disorders such as Alzheimer's, Parkinson's, and cardiovascular diseases. Here we report the design and synthesis of a family of steroid–quinoline hybrid compounds based on the framework combination approach. This set of hybrid compounds effectively inhibited Aβ1–42 self-aggregation *in vitro* by delaying the exponential growth phase and/or reducing the quantity of fibrils in the steady state. Their disaggregation efficacy was further demonstrated against preaggregated Aβ1–42 peptides in cellular assays upon their endocytosis by neuroblastoma cells, as they reverted both the number and the average area of fibrils back to basal levels. The antiaggregation effect of these hybrids was further tested and demonstrated in a cellular model of general protein aggregation expressing a protein aggregation fluorescent sensor. Together, our results show that the new cholesterol–quinoline hybrids possess wide and marked disaggregation capacities and are therefore promising templates for the development of new drugs to deal with conformational disorders.

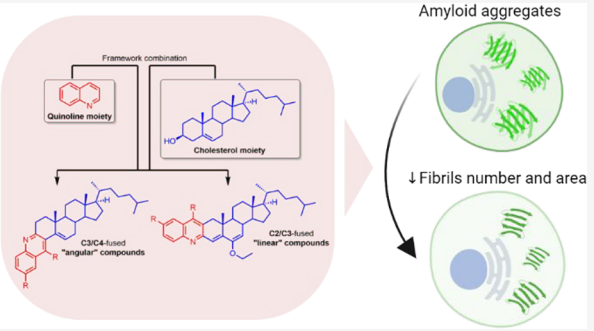

KEYWORDS: *Steroid–quinoline hybrids, protein aggregation, amyloid-β (Aβ) peptide, protein misfolding diseases*

Protein aggregation is the process by which misfolded proteins adopt conformational changes that convert them from a physiologically soluble monomeric form into oligomeric and fibrillar forms, usually ones that are rich in stable β-sheet regions.[1,2] Many neurodegenerative diseases, such as Alzheimer's disease (AD), Huntington's disease, Parkinson's disease (PD), and prion diseases, as well as cardiovascular diseases (atherosclerosis, heart failure, and ischemic heart disease) are associated with protein aggregation. In some of these, smaller oligomeric forms of misfolded (amyloidogenic) proteins have been implicated as a causative agent.[3−5] Although this is not yet fully understood, over the last decades several efforts have been made to understand the molecular processes at the basis of such pathological aggregation by studying their formation and the complex network of chaperones, proteasome, and other regulatory molecules involved in their clearance.[6] These efforts have led to the development of several compounds, including natural products, peptides, and synthetic small molecules, to target many types of protein aggregation.[7,8] In recent years, steroids have emerged as alternative compounds to target not only amyloid-β (Aβ) aggregation but also other protein aggregation processes.[9−11] The seminal example is lanosterol, which because of its amphipathic nature binds to the hydrophobic sites of protein aggregates and exposes its hydrophilic part, causing lanosterol-bound proteins to be more soluble in water.[10,11] These features allow lanosterol to dissociate mutant cellular crystallin aggregates and to inhibit the self-assembly of Aβ entangling with peptides and interfering with the steric zipper interaction at the β-sheet–β-sheet interface.[9,11] In the last case, cholesterol was shown to be less efficient in the inhibition of Aβ aggregation because of its lower hydrophobicity compared with lanosterol.[9] Having that in mind, we focused our attention on the cholesterol molecule (which is readily available and much cheaper than lanosterol) and introduced chemical modifications on it to prepare hybrid cholesterol derivatives. Since quinolines have often been reported as good inhibitors of several types of protein aggregation processes, including Aβ aggregation,[12−18] we

Received: October 30, 2021
Accepted: February 8, 2022
Published: February 14, 2022

https://doi.org/10.1021/acsmedchemlett.1c00604
ACS Med. Chem. Lett. 2022, 13, 443–448

decided to fuse them to cholesterol, expecting to observe a synergic effect of the quinoline and steroid scaffolds (Figure 1).

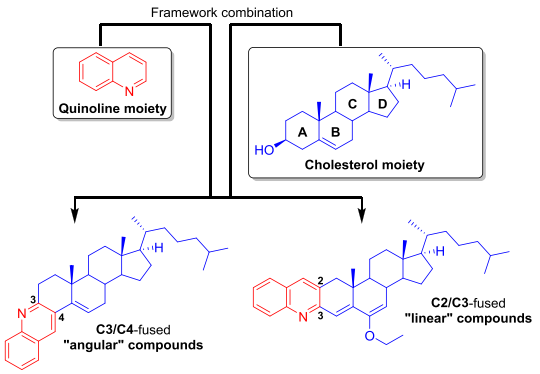

Figure 1. Framework combination to prepare "angular" and "linear" quinoline−steroid hybrids.

As we also introduced aromatic rings, the final hybrids were expected to be more hydrophobic than their cholesterol precursor (Figure 1). In addition, quinolines are also very interesting scaffolds for the development of fluorescent staining diagnostic tools for Aβ, tau, and PrP^{Sc} fibrils, as they are appealing binders of both amyloid and prion fibrils.[14,19−21] With this "framework combination" strategy, which was successfully applied previously to novel anticancer agents,[22] the hybrid compounds (Figure 1) will have aromatic/hydrophobic areas and hydrogen-bonding components, which are common structural features found in most Aβ inhibitors.[8]

The quinoline moiety was arranged within the hybrid compounds in distinct manners to afford "linear" and "angular" compounds, which are fused at the C2/C3 and C3/C4 sides of steroid A ring, respectively (Figure 1).

Compounds **4a−d** and **6a−d** were synthesized following a similar strategy, but the two series started with different oxysteroid precursors (Scheme 1). Compounds **4a−d** were prepared in two steps: (1) Oppenauer oxidation of the 3-OH of cholesterol (**1**) with aluminum isopropoxide [$Al(O^iPr)_3$] to give cholest-4-en-3-one (**2**) in 85% yield (Scheme 1(i))[23] and (2) microwave-assisted Friedlander annulation between **2** and 2′-aminoketones **3a−d** to afford steroid−quinoline hybrid "angular" compounds **4a−d** in 60−85% yield (Scheme 1(ii)).[24] The synthesis of the "linear" compounds **6a−d** followed a similar two-step synthetic approach, differing only in the use of the oxysteroid precursor cholest-4-en-3,6-dione (**5**), which was prepared by oxidation of **1** with pyridinium chlorochromate (PCC) (Scheme 1(iii)).[25] Dione **5** was used as the substrate for the Friedlander reaction with 2′-aminoketones **3a−d**, affording quinoline−cholesterol hybrids **6a−d** in 55−64% yield (Scheme 1(ii)).[24] The structures of the target compounds were fully elucidated using ^1H and ^{13}C NMR spectroscopy and high-resolution mass spectrometry for all compounds and single-crystal X-ray diffraction for compound **4c**, which confirmed the "angular" orientation of the quinoline moiety (see the Supporting Information (SI) for full details) and the retention of the configurations of all asymmetric carbons and the position of the B-ring C5═C6 double bond of the cholesterol moiety.

Scheme 1. Synthesis of Hybrid Compounds 4a−d and 6a−d[a] and (inset) Crystal Structure of 4c

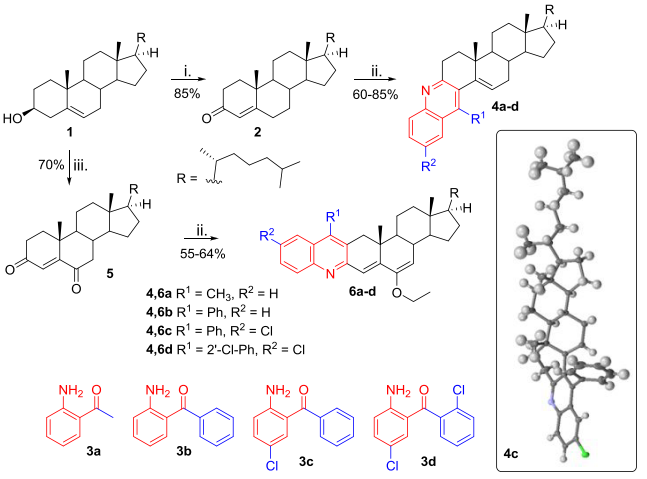

[a]Reagents and conditions: (i) $Al(O^iPr)_3$, cyclohexanone, toluene, reflux, 12 h; (ii) **3a−d**, *p*-TsOH, EtOH, MW, 100 °C, 15 min; (iii) PCC, CH_2Cl_2, rt, 24 h.

With all of the desired compounds prepared, we first investigated their biocompatibility with human cells using the reversible resazurin (alias alamarBlue) metabolic colorimetric viability assay.[26,27] The cytotoxicities of compounds **4a−d** and **6a−d** were assessed in HeLa cells exposed for 24 and 48 h to increasing concentrations. All of the compounds were found to be nontoxic or showed low toxicity at 24 and/or 48 h of exposure at 0.1, 1, 10, 50, and 100 μM (see SI for full details).

The activities of compounds **4a−d** and **6a−d** on the target protein aggregates were then investigated. First, we investigated the effects of compounds **4a−d** and **6a−d** on Aβ1−42 peptide aggregation by a thioflavin-T (ThT) fluorescence assay using quercetin as the positive control (Figure S24).[28] According to the fluorescence intensity curves (Figure 2), the fibrillation process of Aβ1−42 peptides (control) followed a standard nucleated-growth mechanism, defined by a lag phase, a rapid exponential growth phase, and a final equilibrium steady state. Once compounds **4a−d** and **6a−d** were introduced to the monomer peptide solution, the final fluorescence intensity was reduced, indicating inhibition of the aggregation of Aβ1−42 peptides (Figure 2). The single exception was derivative **6d**, which showed no effect on the aggregation of Aβ1−42 peptides. Deserved highlight should be given to derivatives **4d** and **6a**, with which the final fluorescence intensity was greatly reduced, indicating a high degree of aggregation inhibition (Figure 2). On the other hand, for derivatives **4b**, **4c**, **6b**, and **6c**, the reduction of the final fluorescence intensity was mild, suggesting relatively weaker inhibition of peptide aggregation (Figure 2).

The arrangement of the quinoline moiety within the hybrid compounds **4b**, **4c**, **6b**, and **6c** seems to be irrelevant for the inhibition of peptide aggregation, with no relevant differences in their fibrillation processes (Figure S24). On the other hand, for compounds **4a**, **4d**, **6a**, and **6d**, the quinoline arrangement apparently had huge effect on the inhibition of peptide aggregation (Figure S24). The simplest linear compound **6a** demonstrated the highest inhibition effect, closely followed by the angular compound **4d** (Figure S24).

The disaggregation capacities of compounds **4a−d** and **6a−d** were then examined in SH-SY5Y neuronal-like cells incubated with preaggregated synthetic peptide Aβ1−

https://doi.org/10.1021/acsmedchemlett.1c00604
ACS Med. Chem. Lett. 2022, 13, 443−448

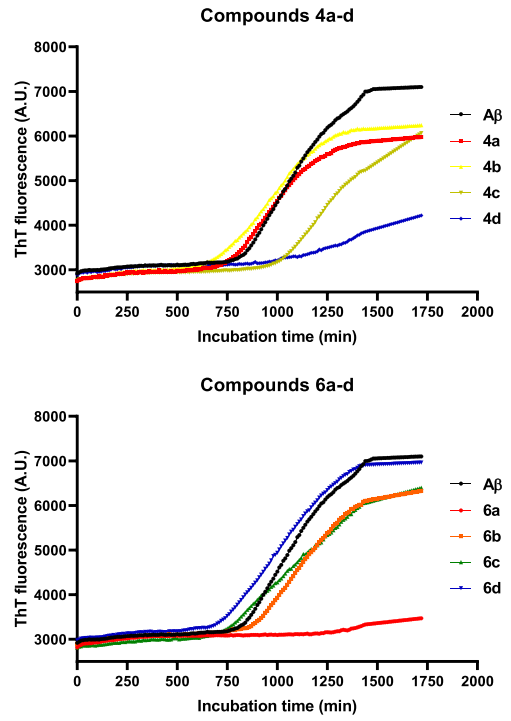

Figure 2. Influence of compounds **4a−d** and **6a−d** (20 μM) on fibrillation of Aβ1−42 peptides (10 μM) monitored by ThT fluorescence. Data are presented as the mean of three experiments (n = 3).

42.[29−31] After incubation with the aggregated Aβ1−42 peptides for 16 h, the cells were further incubated with each compound at 50 μM for an additional 12 h. Following incubation, the cells were fixed, stained with Proteostat protein aggregation assay,[32] and analyzed by confocal microscopy to determine whether there was a decrease in Aβ1−42 staining upon incubation with the tested compounds (Figure 3; see the SI for details). After incubation with the aggregated form of Aβ1−42, numerous red-fluorescent foci were detected throughout the cytoplasm (~4-fold increase relative to the control cells that were in the presence of cellular medium only). An ~5-fold increase in the average area of the foci was also observed, suggesting this as a suitable cellular model to screen the ability of compounds to disaggregate Aβ1−42 fibrils. Generally, the compounds were able to decrease the number of foci to basal levels, with the exceptions of derivatives **4c** and **6b**, which caused a large increase in the number of foci in comparison with Aβ1−42-incubated cells (Figure 3A). On the other hand, the average area of the foci was significantly reduced only in the presence of compounds **4c**, **6a**, **6c**, and **6d** (Figure 3B). The remaining compounds did not show any meaningful effect on the area of the foci, with the exception of **6b**, which caused an increase in the average area (Figure 3B). Figure 3C shows examples of confocal microscopy images for representative compounds **4c** and **6c**, in which one can observe a high number of red foci for compound **4c**, in contrast with compound **6c**.

Besides Aβ1−42 fibril formation, which is a hallmark of AD, there are various physiological- and pathological-relevant stresses that impact cell proteostasis and induce general protein aggregation. To mimic conditions of general protein aggregation and to test the ability of our synthetic compounds to reverse the random aggregation process, we used nilotinib

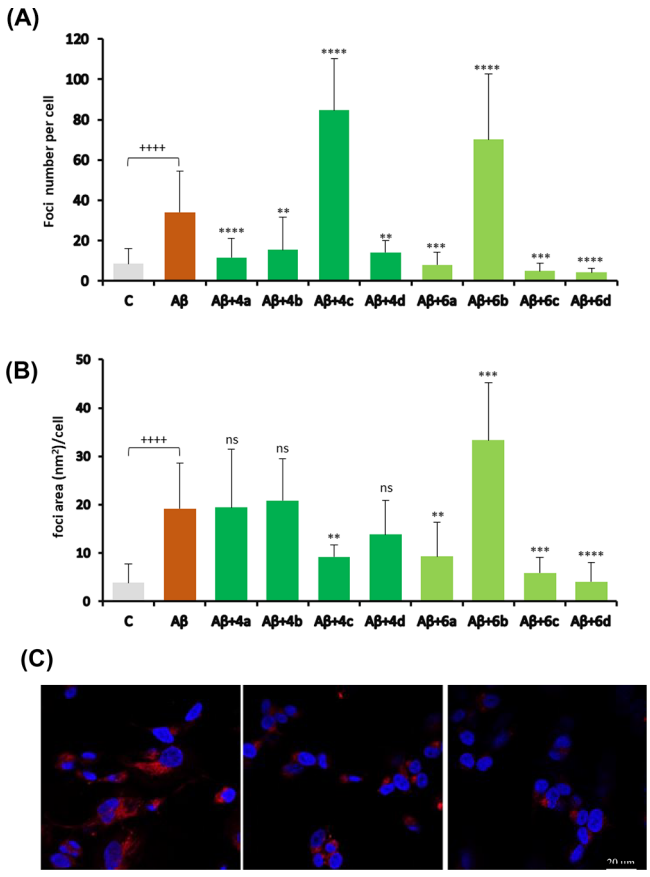

Figure 3. Evaluation of compounds' disaggregation effect in SH-SY5Y cells incubated with preaggregated Aβ1−42. (A) Numbers of protein aggregate foci per cell. (B) Average areas of protein aggregate foci per cell. Both control and Aβ-exposed cells were incubated in the presence of 0.5% EtOH (compound vehicle). Data are presented as mean ± SD (10−20 fields of view, n = 2, average of ~370 cells analyzed per condition). Significance was determined using the unpaired Student's t test: (+) for comparison between positive (Aβ) and negative (C) control conditions and (*) for comparison between Aβ and Aβ + compounds. +/*, $p < 0.05$; ++/**, $p < 0.01$; +++/***, $p < 0.001$; ++++/****, $p < 0.0001$. (C) Micrographs of cells incubated with Aβ1−42 alone (left) or in combination with compound **4c** (center) or **6c** (right).

(NTB), a clinically used anticancer drug that inhibits the tyrosine kinase protein Bcr-Abl[33,34] and induces proteostasis impairments, being employed to test protein aggregation sensors.[35,36] The disaggregation potential of the synthesized compounds was studied by incubating HeLa cells expressing the protein aggregation sensor HSP27:GFP[37] with NTB in the presence or absence of the tested compounds. Under protein-misfolding conditions, the HSP27:GFP sensor is relocalized to foci in cells, which can be detected by fluorescence microscopy.[37] If the tested compounds have the ability to disaggregate the misfolded proteins generated upon incubation with NTB, a decrease in the number and/or size of the HSP27:GFP foci will be detected (see the SI for details). To evaluate the disaggregation ability of compounds **4a−d** and **6a−d**, HSP27:GFP HeLa cells were incubated for 48 h with 5 μM NTB and coincubated with compounds **4a−d** and **6a−d** at 50 μM in the last 12 h of the incubation period. The assay outputs (number and area of protein aggregate foci per cell) are presented in Figure 4A,B. NTB increased the average number of cellular protein aggregates more than 5-fold, from

https://doi.org/10.1021/acsmedchemlett.1c00604
ACS Med. Chem. Lett. 2022, 13, 443−448

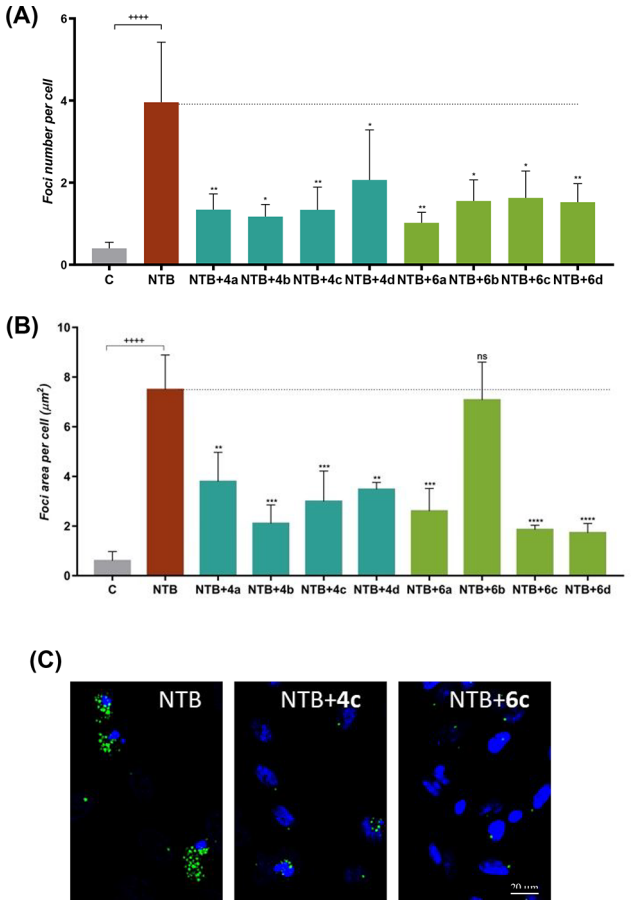

Figure 4. Analyses of the disaggregation capacities of compounds **4a–d** and **6a–d** under conditions of general protein aggregation. (A) Numbers and (B) average areas of green-fluorescing foci of protein aggregates per cell. Control and NTB-exposed cells were grown in the presence of 0.5% EtOH (compound vehicle). Data are presented as mean ± SD (n = 4–10, average of a total of ∼4700 cells analyzed per condition). Significance was determined using the unpaired Student's t test: (+) for comparison between positive (NTB) and negative (C) control conditions and (*) for comparison between NTB and NTB + compounds. +/*, $p < 0.05$; ++/**, $p < 0.01$; +++/***, $p < 0.001$; ++++/****, $p < 0.0001$. (C) Micrographs of representative cells of compounds **4c** and **6c**. Aggregates are in green (HSP27:GFP fusion protein) and cell nuclei in blue (DAPI).

0.71 ± 0.30 to 3.96 ± 1.39, as expected since NTB was seen to promote protein aggregation.[35] All of the synthesized compounds were able to significantly reduce the number of NTB-induced protein aggregates by ∼50–75%. The highest capacity was observed for **6a**, while **4d** demonstrated the lowest potential for decreasing the number of foci (Figure 4A). NTB also highly increased the average area of protein aggregates per cell (Figure 4B) by a factor of 12.5, from 0.6 ± 0.3 to 7.5 ± 1.3 μm^2. All of the synthesized compounds except **6b** were able to significantly reduce the area of NTB-induced protein aggregates, again by ∼50–75%. Compounds **6c** and **6d** showed the highest ability to reduce the area of the aggregates. Representative cells from NTB + **4c** and NTB + **6c** conditions are shown in Figure 4C.

In summary, eight new hybrid compounds designed by framework combination of quinoline and cholesterol scaffolds were synthesized and proved capable of inhibiting and reversing different types of protein aggregation. With this work, we found evidence that cholesterol could be used as template to create new compounds to deal with protein aggregation processes. The previously reported weaker suppressing effect of cholesterol on Aβ peptide aggregation was overcome by framework combination with a quinoline moiety. Our discovery is in line with previous conclusions demonstrating that compounds with higher hydrophobicity are better binders of Aβ oligomers. This hybridization strategy also proved capable of reversing general protein aggregation processes induced by nilotinib and might be interesting to deal with protein-misfolding diseases.

■ ASSOCIATED CONTENT

Supporting Information

The Supporting Information is available free of charge at https://pubs.acs.org/doi/10.1021/acsmedchemlett.1c00604.

Spectra, biological assay data, and experimental procedures (PDF)

■ AUTHOR INFORMATION

Corresponding Author

Artur M. S. Silva − *LAQV-REQUIMTE, Department of Chemistry, University of Aveiro, 3810-193 Aveiro, Portugal;* orcid.org/0000-0003-2861-8286; Phone: +351-234-370714; Email: artur.silva@ua.pt

Authors

Hélio M. T. Albuquerque − *LAQV-REQUIMTE, Department of Chemistry, University of Aveiro, 3810-193 Aveiro, Portugal*

Raquel Nunes da Silva − *LAQV-REQUIMTE, Department of Chemistry, University of Aveiro, 3810-193 Aveiro, Portugal; Department of Medical Sciences and Institute of Biomedicine, IBiMED, University of Aveiro, 3810-193 Aveiro, Portugal*

Marisa Pereira − *Department of Medical Sciences and Institute of Biomedicine, IBiMED, University of Aveiro, 3810-193 Aveiro, Portugal*

André Maia − *Instituto de Investigação e Inovação em Saúde (i3S) and Instituto de Biologia Molecular e Celular (IBMC), Universidade do Porto, 4200-135 Porto, Portugal*

Samuel Guieu − *LAQV-REQUIMTE, Department of Chemistry, University of Aveiro, 3810-193 Aveiro, Portugal; CICECO Aveiro-Institute of Materials and Department of Chemistry, University of Aveiro, 3010-193 Aveiro, Portugal;* orcid.org/0000-0002-7439-209X

Ana Raquel Soares − *Department of Medical Sciences and Institute of Biomedicine, IBiMED, University of Aveiro, 3810-193 Aveiro, Portugal*

Clementina M. M. Santos − *LAQV-REQUIMTE, Department of Chemistry, University of Aveiro, 3810-193 Aveiro, Portugal; Centro de Investigação de Montanha (CIMO), Instituto Politécnico de Bragança, 5300-252 Bragança, Portugal*

Sandra I. Vieira − *Department of Medical Sciences and Institute of Biomedicine, IBiMED, University of Aveiro, 3810-193 Aveiro, Portugal*

Complete contact information is available at: https://pubs.acs.org/10.1021/acsmedchemlett.1c00604

Author Contributions

#H.M.T.A. and R.N.d.S. contributed equally. The manuscript was written through contributions of all authors. All of the authors approved the final version of the manuscript.

Notes

The authors declare no competing financial interest.

■ ACKNOWLEDGMENTS

Thanks are due to the University of Aveiro, FCT/MEC, Centro 2020 and Portugal2020, the COMPETE Program, and the European Union (FEDER Program) via the financial support to the research units LAQV-REQUIMTE (UIDB/50006/2020), IBiMED (UID/BIM/04501/2019) and CICECO-Aveiro Institute of Materials (UID/CTM/50011/2019), financed by national funds through the FCT/MCTES, to the Portuguese NMR Network, to the ThiMES Project (POCI-01-0145-FEDER-016630), and to the PAGE Project "Protein Aggregation Across the Lifespan" (CENTRO-01-0145-FEDER-000003), including postdoctoral grants to H.M.T.A. (BPD/UI98/4861/2017) and R.N.d.S. (BPD/UI98/6327/2018). M.P. was supported by Ph.D. Grant SFRH/BD/135655/2018. A.R.S. and S.G. were supported by national funds (OE) through FCT, I.P., in the scope of the framework contract foreseen in numbers 4, 5, and 6 of Article 23 of the Decree-Law 57/2016 of August 29, changed by Law 57/2017 of July 19. Microphotographs were acquired in the LiM facility of iBiMED/UA, a member of the Portuguese Platform of BioImaging (PPBI) (POCI-01-0145-FEDER-022122).

■ ABBREVIATIONS

AD, Alzheimer's disease; PD, Parkinson's disease; PrP^{Sc}, scrapie prion protein; PCC, pyridinium chlorochromate; $Al(O^iPr)_3$, aluminum isopropoxide; *p*-TsOH, *p*-toluenesulfonic acid; ThT, thioflavin-T; NTB, nilotinib; HSP27:GFP, heat shock protein 27:green fluorescent protein

■ REFERENCES

(1) Alam, P.; Siddiqi, K.; Chturvedi, S. K.; Khan, R. H. Protein aggregation: From background to inhibition strategies. *Int. J. Biol. Macromol.* **2017**, *103*, 208−219.

(2) Chiti, F.; Dobson, C. M. Protein misfolding, amyloid formation, and human disease: A summary of progress over the last decade. *Annu. Rev. Biochem.* **2017**, *86*, 27−68.

(3) Miyazaki, Y.; Mizumoto, K.; Dey, G.; Kudo, T.; Perrino, J.; Chen, L.-c.; Meyer, T.; Wandless, T. J. A method to rapidly create protein aggregates in living cells. *Nat. Commun.* **2016**, *7* (1), 11689.

(4) Kreutzer, A. G.; Nowick, J. S. Elucidating the structures of amyloid oligomers with macrocyclic β-hairpin peptides: Insights into Alzheimer's disease and other amyloid diseases. *Acc. Chem. Res.* **2018**, *51* (3), 706−718.

(5) Arrasate, M.; Finkbeiner, S. Protein aggregates in Huntington's disease. *Exp. Neurol.* **2012**, *238* (1), 1−11.

(6) Eisele, Y. S.; Monteiro, C.; Fearns, C.; Encalada, S. E.; Wiseman, R. L.; Powers, E. T.; Kelly, J. W. Targeting protein aggregation for the treatment of degenerative diseases. *Nat. Rev. Drug Discovery* **2015**, *14*, 759.

(7) Lashuel, H. A. Rethinking protein aggregation and drug discovery in neurodegenerative diseases: Why we need to embrace complexity? *Curr. Opin. Chem. Biol.* **2021**, *64*, 67−75.

(8) Malafaia, D.; Albuquerque, H. M. T.; Silva, A. M. S. Amyloid-β and tau aggregation dual-inhibitors: A synthetic and structure-activity relationship focused review. *Eur. J. Med. Chem.* **2021**, *214*, 113209.

(9) Zhou, H.; Yang, Z.; Tian, X.; Chen, L.; Lee, S.; Huynh, T.; Ge, C.; Zhou, R. Lanosterol disrupts the aggregation of amyloid-β peptides. *ACS Chem. Neurosci.* **2019**, *10* (9), 4051−4060.

(10) Zhao, L.; Chen, X.-J.; Zhu, J.; Xi, Y.-B.; Yang, X.; Hu, L.-D.; Ouyang, H.; Patel, S. H.; Jin, X.; Lin, D.; Wu, F.; Flagg, K.; Cai, H.; Li, G.; Cao, G.; Lin, Y.; Chen, D.; Wen, C.; Chung, C.; Wang, Y.; Qiu, A.; Yeh, E.; Wang, W.; Hu, X.; Grob, S.; Abagyan, R.; Su, Z.; Tjondro, H. C.; Zhao, X.-J.; Luo, H.; Hou, R.; Jefferson, J.; Perry, P.; Gao, W.; Kozak, I.; Granet, D.; Li, Y.; Sun, X.; Wang, J.; Zhang, L.; Liu, Y.; Yan, Y.-B.; Zhang, K. Lanosterol reverses protein aggregation in cataracts. *Nature* **2015**, *523*, 607.

(11) Yang, X.; Chen, X.-J.; Yang, Z.; Xi, Y.-B.; Wang, L.; Wu, Y.; Yan, Y.-B.; Rao, Y. Synthesis, evaluation, and structure−activity relationship study of lanosterol derivatives to reverse mutant-Crystallin-induced protein aggregation. *J. Med. Chem.* **2018**, *61* (19), 8693−8706.

(12) Navarrete, L. P.; Guzman, L.; San Martin, A.; Astudillo-Saavedra, L.; Maccioni, R. B. Molecules of the quinoline family block tau self-aggregation: implications toward a therapeutic approach for Alzheimer's disease. *J. Alzheimer's Dis.* **2012**, *29* (1), 79−88.

(13) Camps, P.; Formosa, X.; Galdeano, C.; Munoz-Torrero, D.; Ramirez, L.; Gomez, E.; Isambert, N.; Lavilla, R.; Badia, A.; Clos, M. V.; Bartolini, M.; Mancini, F.; Andrisano, V.; Arce, M. P.; Rodriguez-Franco, M. I.; Huertas, O.; Dafni, T.; Luque, F. J. Pyrano[3,2-c]quinoline-6-chlorotacrine hybrids as a novel family of acetylcholinesterase- and beta-amyloid-directed anti-Alzheimer compounds. *J. Med. Chem.* **2009**, *52* (17), 5365−79.

(14) Li, Y.; Chen, C.; Xu, D.; Poon, C.-Y.; Ho, S.-L.; Zheng, R.; Liu, Q.; Song, G.; Li, H.-W.; Wong, M. S. Effective theranostic cyanine for imaging of amyloid species in vivo and cognitive improvements in mouse model. *ACS Omega* **2018**, *3* (6), 6812−6819.

(15) Chen, X.; Wehle, S.; Kuzmanovic, N.; Merget, B.; Holzgrabe, U.; König, B.; Sotriffer, C. A.; Decker, M. Acetylcholinesterase inhibitors with photoswitchable inhibition of β-amyloid aggregation. *ACS Chem. Neurosci.* **2014**, *5* (5), 377−389.

(16) Wang, Z.; Hu, J.; Yang, X.; Feng, X.; Li, X.; Huang, L.; Chan, A. S. C. Design, synthesis, and evaluation of orally bioavailable quinoline−indole derivatives as innovative multitarget-directed ligands: Promotion of cell proliferation in the adult murine hippocampus for the treatment of Alzheimer's disease. *J. Med. Chem.* **2018**, *61* (5), 1871−1894.

(17) Kim, B.; Park, H.; Lee, S. K.; Park, S. J.; Koo, T.-S.; Kang, N. S.; Hong, K. B.; Choi, S. Systemic optimization and structural evaluation of quinoline derivatives as transthyretin amyloidogenesis inhibitors. *Eur. J. Med. Chem.* **2016**, *123*, 777−787.

(18) Yue, X.; Dhavale, D. D.; Li, J.; Luo, Z.; Liu, J.; Yang, H.; Mach, R. H.; Kotzbauer, P. T.; Tu, Z. Design, synthesis, and in vitro evaluation of quinolinyl analogues for α-synuclein aggregation. *Bioorg. Med. Chem. Lett.* **2018**, *28* (6), 1011−1019.

(19) Staderini, M.; Aulić, S.; Bartolini, M.; Tran, H. N. A.; González-Ruiz, V.; Pérez, D. I.; Cabezas, N.; Martínez, A.; Martín, M. A.; Andrisano, V.; Legname, G.; Menéndez, J. C.; Bolognesi, M. L. A fluorescent styrylquinoline with combined therapeutic and diagnostic activities against Alzheimer's and prion diseases. *ACS Med. Chem. Lett.* **2013**, *4* (2), 225−229.

(20) Li, Y.; Xu, D.; Ho, S. L.; Li, H. W.; Yang, R.; Wong, M. S. A theranostic agent for in vivo near-infrared imaging of beta-amyloid species and inhibition of beta-amyloid aggregation. *Biomaterials* **2016**, *94*, 84−92.

(21) Li, Y.; Xu, D.; Sun, A.; Ho, S.-L.; Poon, C.-Y.; Chan, H.-N.; Ng, O. T. W.; Yung, K. K. L.; Yan, H.; Li, H.-W.; Wong, M. S. Fluoro-substituted cyanine for reliable in vivo labelling of amyloid-β oligomers and neuroprotection against amyloid-β induced toxicity. *Chem. Sci.* **2017**, *8* (12), 8279−8284.

(22) Baji, Á.; Gyovai, A.; Wölfling, J.; Minorics, R.; Ocsovszki, I.; Zupkó, I.; Frank, É. Microwave-assisted one-pot synthesis of steroid−quinoline hybrids and an evaluation of their antiproliferative activities on gynecological cancer cell lines. *RSC Adv.* **2016**, *6* (33), 27501−27516.

(23) Amr, A.-G. E.; Abdulla, M. M. Anti-inflammatory profile of some synthesized heterocyclic pyridone and pyridine derivatives fused with steroidal structure. *Bioorg. Med. Chem.* **2006**, *14* (13), 4341−4352.

(24) Jia, C. S.; Zhang, Z.; Tu, S. J.; Wang, G. W. Rapid and efficient synthesis of poly-substituted quinolines assisted by p-toluene sulphonic acid under solvent-free conditions: comparative study of

https://doi.org/10.1021/acsmedchemlett.1c00604
ACS Med. Chem. Lett. 2022, 13, 443−448

microwave irradiation versus conventional heating. *Org. Biomol. Chem.* **2006**, *4* (1), 104−10.
(25) Cui, J.; Wang, H.; Huang, Y.; Xin, Y.; Zhou, A. Synthesis and cytotoxic analysis of some disodium 3*β*,6*β*-dihydroxysterol disulfates. *Steroids* **2009**, *74* (13), 1057−1060.
(26) Prabst, K.; Engelhardt, H.; Ringgeler, S.; Hubner, H. Basic colorimetric proliferation assays: MTT, WST, and resazurin. *Methods Mol. Biol.* **2017**, *1601*, 1−17.
(27) Pina, S.; Vieira, S. I.; Torres, P. M. C.; Goetz-Neunhoeffer, F.; Neubauer, J.; da Cruz e Silva, O. A. B.; da Cruz e Silva, E. F.; Ferreira, J. M. F. In vitro performance assessment of new brushite-forming Zn- and ZnSr-substituted beta-TCP bone cements. *J. Biomed. Mater. Res., Part B* **2010**, *94B* (2), 414−420.
(28) Murakami, K.; Yoshioka, T.; Horii, S.; Hanaki, M.; Midorikawa, S.; Taniwaki, S.; Gunji, H.; Akagi, K.-i.; Kawase, T.; Hirose, K.; Irie, K. Role of the carboxy groups of triterpenoids in their inhibition of the nucleation of amyloid *β*42 required for forming toxic oligomers. *Chem. Commun.* **2018**, *54* (49), 6272−6275.
(29) Henriques, A. G.; Vieira, S. I.; Crespo-López, M. E.; Guiomar de Oliveira, M. A.; da Cruz e Silva, E. F.; da Cruz e Silva, O. A. B. Intracellular sAPP retention in response to A*β* is mapped to cytoskeleton-associated structures. *J. Neurosci. Res.* **2009**, *87* (6), 1449−1461.
(30) Wesén, E.; Jeffries, G. D. M.; Matson Dzebo, M.; Esbjörner, E. K. Endocytic uptake of monomeric amyloid-*β* peptides is clathrin- and dynamin-independent and results in selective accumulation of A*β*(1−42) compared to A*β*(1−40). *Sci. Rep.* **2017**, *7* (1), 2021.
(31) Henriques, A. G.; Vieira, S. I.; Da Cruz e Silva, E. F.; Da Cruz e Silva, O. A. B. A*β* promotes Alzheimer's disease-like cytoskeleton abnormalities with consequences to APP processing in neurons. *J. Neurochem.* **2010**, *113* (3), 761−771.
(32) Cheng, S.; Banerjee, S.; Daiello, L. A.; Nakashima, A.; Jash, S.; Huang, Z.; Drake, J. D.; Ernerudh, J.; Berg, G.; Padbury, J.; Saito, S.; Ott, B. R.; Sharma, S. Novel blood test for early biomarkers of preeclampsia and Alzheimer's disease. *Sci. Rep.* **2021**, *11* (1), 15934.
(33) Jabbour, E.; Cortes, J.; Kantarjian, H. Nilotinib for the treatment of chronic myeloid leukemia: An evidence-based review. *Core Evidence* **2009**, *4*, 207−213.
(34) Breccia, M.; Alimena, G. Nilotinib: A second-generation tyrosine kinase inhibitor for chronic myeloid leukemia. *Leuk. Res.* **2010**, *34* (2), 129−134.
(35) Liu, Y.; Fares, M.; Dunham, N. P.; Gao, Z.; Miao, K.; Jiang, X.; Bollinger, S. S.; Boal, A. K.; Zhang, X. AgHalo: A facile fluorogenic sensor to detect drug-induced proteome stress. *Angew. Chem., Int. Ed.* **2017**, *56* (30), 8672−8676.
(36) Lekes, D.; Szadvari, I.; Krizanova, O.; Lopusna, K.; Rezuchova, I.; Novakova, M.; Novakova, Z.; Parak, T.; Babula, P. Nilotinib induces ER stress and cell death in H9c2 cells. *Physiol. Res.* **2016**, *65*, S505−S514.
(37) Pereira, M.; Tomé, D.; Domingues, A. S.; Varanda, A. S.; Paulo, C.; Santos, M. A. S.; Soares, A. R. A fluorescence-based sensor assay that monitors general protein aggregation in human cells. *Biotechnol. J.* **2018**, *13* (4), 1700676.

https://doi.org/10.1021/acsmedchemlett.1c00604
ACS Med. Chem. Lett. 2022, 13, 443−448